



ISSN: 0067-2904

# TiO<sub>2</sub>: CuO and TiO<sub>2</sub>: ZnO/ paraffin wax as Nano composites: synthesis and investigation as solar energy cells and corrosion inhibitors.

## Tabarak saad hasan\*, Basim Ibrahim Al-Abdaly

Department of Chemistry, College of Science, University of Baghdad, Baghdad, Iraq

Received: 5/11/2023 Accepted: 22/8/2024 Published: 30/8/2025

#### **ABSTRACT**

In this study, nanoparticles of the metal oxides CuO, ZnO, and TiO<sub>2</sub> were synthesized using the hydrothermal method. These nanoparticles were then used to dope paraffin wax (as the matrix material) and prepare nanocomposites [TiO<sub>2</sub>; CuO/paraffin] and [TiO2; ZnO/paraffin] through the ultrasound method. The morphology, size, and structures of the synthesized nanocomposite were examined and characterized using atomic force microscopy (AFM), X-ray diffraction (XRD), Fourier and transform infrared (FT-IR), in order to confirm the design of nanocomposite based nanostructures and reveal their distinctive features from where distribution on paraffin wax. The results of AFM analysis of the two synthesized nanostructure, [TiO<sub>2</sub>; CuO/paraffin] and [TiO<sub>2</sub>; ZnO/paraffin], revealed that the size of the nanoparticles was within the nanoscale range, measuring 49.54 nm and 57.16 nm, respectively. Their grooves in all nanostructures of the synthesized composites are heterogeneous as depicted by three-dimensional images, this is mainly caused by the agglomeration of metal oxide nanoparticles which leads to coverage of some of the paraffin surface. The activities of Nano composites synthesized were studied from the industrial side, including solar cell energy and the use of these Nano composites as inhibitors for corrosion. The findings for all of these nanocomposite revealed they have the properties of solar cells and a significant inhibitory effect.

**Keywords:** paraffin wax ,hydrothermal method ,metal oxide , ultra-sonic method, doping.

ثنائي اوكسيد التيتانيوم مع اوكسيد النحاس وثنائي اوكسيد التيتانيوم مع اوكسيد الزك المشوبان مع شمع البارافين تحضيرهم كمركبات نانوبة والتحقيق كخلايا طاقة شمسية ومثبطات للتآكل

> تبارك سعد حسن \*، باسم ابراهيم العبدلي قسم علوم الكيمياء , كلية العلوم ,جامعة بغداد , بغداد , العراق

#### الخلاصة

في هذه الدراسة ، تم تحضير الجسيمات النانوبة لأكاسيد المعادن CuO و ZnO و TiO<sub>2</sub> باستخدام الطريقة الحرارية المائية. ثم تم استخدام هذه الجسيمات النانوية لتشويب شمع البارافين (كمادة مصفوفة) وإعداد المركبات النانوية [/TiO2; CuO/ابارافين] و TiO2; ZnO / البارافين] من خلال طريقة الموجات فوق الصوتية. تم فحص مورفولوجيا وججم وهياكل المركبات النانوبة المركبة وتوصيفها باستخدام مجهر القوة الذربة

\*Email: totasaad929@gmail.com

(AFM) وحيود الأشعة السينية (XRD) وفورييه وتحويل الأشعة تحت الحمراء (FT-IR) ، وذلك لتأكيد تصميم البني النانوية القائمة على المركبات النانوية والكشف عن سماتها المميزة من حيث التوزيع على شمع البارافين. نتائج تحليل AFM للهيكلين النانويين المركبين ، [TiO2; CuO] بالرافين] و [ 57.16 للهيكالين النانويين المركبين ، بقياس 49.54 لانومتر و 57.16 نانومتر على التوالي.. الأخاديد في جميع الهياكل النانوية للمركبات المركبة غير متجانسة كما هو موضح في الصور ثلاثية الأبعاد ، ويرجع ذلك أساسًا إلى تكتل جزيئات أكسيد المعادن النانوية مما يؤدي إلى تغطية بعض سطح البارافين. تمت دراسة أنشطة المركبات النانوية المركبة من الجانب الصناعي ، بما في ذلك طاقة الخلايا الشمسية واستخدام هذه المركبات النانوية كمثبطات للتآكل. كشفت النتائج لجميع هذه المركبات النانوية أن لها خصائص الخلايا الشمسية وتأثير تثبيط كبير.

#### 1.Introduction

"Nano composite" denotes a composite material incorporating a constituent phase with a nanometric morphology, examples including nanoparticles, nanotubes, or layered nanostructures. Since they consist of multiple phases, they are multiphase materials, and at least one of those phases needs to have a diameter between 10 and 100 nm. Nanocomposites have emerged as beneficial replacements for engineering materials that currently have drawbacks. Nanocomposite can be divided into groups based on the elements of their scattered matrix and dispersion phase [1]. The rapidly evolving field of nanotechnology has opened up possibilities to create a wide range of exciting and innovative materials with unique and distinctive properties. Along with their own characteristics, the so-called founds attributes were also strongly influenced by the originals' morphological and interfacial characteristics. Of course, we cannot completely rule out the idea that the parent constituent materials were unaware of the newly developed characteristic in the substance [2,3]. Thus, the concept behind Nano composite is to develop and make new materials that are remarkably adaptable and improved in their physical qualities using building blocks with diameters in the nanoscale range.

Among the studied nanomaterials is wax, which was dealt with at the nanoscale level that is supported in the literature [4], and in this research, we tried to stimulate the properties of this wax by adding nano metal oxides with what is called doping and obtaining new Nanocomposites, where we envisage in this study to improving the properties of wax through the addition of nano metal oxides and the extent to which this addition reflects on the surface and structural properties of wax and its implications for the application of wax in the industrial field as solar cells and as corrosion inhibitors[5].

Nanocomposite have a tremendous amount of potential as high-performance materials because they exhibit unexpected property combinations and distinctive design options. As a result, they are useful in a wide range of industries, from packaging to biomedical applications [6].

Nanocomposite can be fabricated by combining any of the three fundamental components: metals, ceramics, and polymers[7-9]. Thus, the mechanical, electrochemical, electrical, catalytic, thermal, and optical properties of the Nano composite may be combined or be noticeably different from those of the component materials [10].

In this study, we added metal oxides to paraffin wax in order to enhance both the properties of paraffin wax and the performance of the resulting nanocomposites, which were studied from the industrial side, including solar cell energy and the use of these Nano

composites as inhibitors for corrosion. The findings for all of these nanocomposite revealed they have the properties of solar cells and a significant inhibitory effect.

#### 2. Materials and Methods

#### 2.1 Materials

Cupper acetate monohydrate( Cu(CH<sub>3</sub>COO)<sub>2</sub>.H<sub>2</sub>O) , Ammonia hydroxide( NH<sub>4</sub>OH), Sodium hydroxide NaOH, deionized water , zinc acetate dehydrate Zn(CH<sub>3</sub>COO)<sub>2</sub>.2H<sub>2</sub>O), titanium tetra isopropoxide Ti(OCH( CH<sub>3</sub>)<sub>2</sub>)<sub>4</sub> , isopropanol , Distilled water.

#### 2.2 Methods

2.2.1Synthesis of cobalt oxide nanoparticle [CuO] by hydrothermal method [11]. 4g of Cu(CH3COO)2.H2O (serving as the precursor) was dissolved in 30mL of deionized water to prepare a 0.5 M solution (labeled as 1st solution). Subsequently, 3mL of 0.5 M NH4OH was added to the 1st solution. Additionally, 0.2g of NaOH was dissolved in 10mL of deionized water to make a 0.5 M solution (labeled as the 2nd solution). The two solutions were transferred into the Teflon linear autoclave cell, and then the mixture produced is heated at a rate of 2°C/min (around 150 °C) for 12 hours. Centrifuging the product at 4000 rpm for 10 minutes after cooling the cell separated the product. The separated material was then dried at 90°C.

## 2.2.2 Synthesis of Zinc oxide nanoparticle [ZnO] by hydrothermal method [12].

To prepare the solutions, 5.8 grams of zinc acetate dihydrate (Zn(CH3COO)2.2H2O) were dissolved in 25 milliliters of deionized water to create a 0.5 M solution (labeled as 1st solution). Additionally, 0.2 grams of sodium hydroxide (NaOH) were dissolved in 10 milliliters of deionized water to produce a 0.5 M solution (labeled as the 2nd solution). Then, the same procedure in 2.2.1 section was applied.

## 2.2.3 Synthesis of titanium dioxide nanoparticle [ $TiO_2$ ].

In this step, the solvents employed were distilled water, isopropanol, and titanium tetra isopropoxide, the latter functioning as a precursor. Titanium tetra isopropoxide [TTIP] and isopropanol were added to 10 mL of distilled water in a 1:4 molar ratio after which a suspension solution of a white color developed. The mixture was then agitated for an hour to produce a transparent solution. After the solutions were combined, the mixture was transferred into a Teflon-lined autoclave. The autoclave was then heated to approximately 150°C for a duration of 18 hours, with a heating rate of 2°C per minute. Once the autoclave had reached room temperature, the supernatant was removed, and the precipitates were washed repeatedly with distilled water. TiO<sub>2</sub> nanoparticles were dried at 90 °C.

### 2.2.4 Synthesis of Nano composite [TiO<sub>2</sub>;CuO/paraffin] by Ultra-sonic method [13]

The nanoparticles were prepared by dissolving 0.05 mg of copper oxide in 20 mL of deionized water. Similarly, 0.05 mg of titanium dioxide were dissolved in 20 mL of deionized water. Additionally, 0.9 milligrams of paraffin were dissolved in 50 mL of chloroform solvent, resulting in a ratio of 1 part paraffin to 9 parts chloroform. Each solution of nanometal oxide was added slowly (as drops) to the solution of paraffin, Under various conditions (40°C, 1h), mixture was ultrasonically bombarded with a high-density ultrasonic probe inglorious directly into the solution. To achieve the best results, the sonication time was altered. The precipitate developed and was dried at 90°C in an oven for 5 h.

## 2.2.5 Synthesis of nanocomposite [TiO2; ZnO/paraffin] by Ultra-sonic method

Accordingly, 0.05g of zinc oxide nanoparticles were dissolved in 20 mL of deionized water, while 0.05g of titanium oxide nanoparticles were separately dissolved in another 20 mL portion of deionized water. While the organic matter of paraffin (0.9mg) dissolved in 50 mL of chloroform solvent for ratio (1:9), it was carried out by the same method used in the above (2.2.4).

### 2.2.6 Preparation Dye-Sensitized Solar Cell(DSSCs).

## 2.2.6.1 Preparation of (ITO/TiO<sub>2</sub>; CuO-Paraffin) Photo anodes.

To make an active anode, 0.1 g of [TiO<sub>2</sub>;CuO/paraffin] nanoparticles with 10 mL of deionized water and a few drops of diluted acetic acid for 10 minutes. The TiO2;CuO/paraffin paste was applied, distributed, and then covered on the four sides of the indium tin oxide conductive glass (ITO glass) to obtain a uniform layer thickness and an active area of 2 x 1.5 cm<sup>2</sup>. After that, the material was dried at room temperature for 30 minutes, put in a furnace for 60 minutes, pulled out to cool, and then washed with water and ethanol. [ITO/TiO<sub>2</sub>; ZnO/paraffin] photo anodes are prepared using the same process.to prepare other photo anodes of [ITO/TiO<sub>2</sub>;ZnO/paraffin].

## 2.2.6.2 Preparation of Pt/ITO Cathodic Electrodes

Chemical deposition is used to deposit platinum Pt on ITO conductive glass in order to create a Pt counter electrode. Drops of chloroplatinic acid (5 mM) are added to the glass, which is then heated at 400 °C for 30 minutes before cooling to room temperature. before cooling to room temperature. By adding a few drops of (I-/I\_3-) electrolyte to ITO/TiO<sub>2</sub> and [TiO<sub>2</sub>;CuO/paraffin] placed on ITO glass, which served as the photo-anode, the DSSCs were assembled. A hot melt gasket was used to link the two electrodes face to face. The DSSC's parts were set up in a sandwich-like arrangement.

#### 3. Results and Discussion

### 3.1 Characterization

3.1.1(FT-IR) spectral data for nanocomposite [TiO2; CuO/paraffin] by Ultra-sonic method. FT-IR spectroscopy is a valuable analytical technique for identifying unknown specimens and providing insights into the molecular composition and chemical bonding of both inorganic and organic materials. The various absorption peaks in the FT-IR spectrum, which are associated with the production of atomic bonds and particular frequencies, provide molecular information about the material as [CuO/paraffin] [14]. The FT-IR spectrum of nanocomposite is shown in (see Figure.1). The bands at 3743 cm<sup>-1</sup> (the vibratory stretch of OH), 3359 cm<sup>-1</sup> (stretching vibration of C-H group), 1691 cm<sup>-1</sup> (bending vibration C=C), 1465 cm<sup>-1</sup> (CH3 scissoring motion) and 1118 cm-1 (C-O-C stretch vibration) were observed. The characteristic band of nanoparticles CuO is found lightly shifted to the lower frequency at 518 cm<sup>-1</sup> [15]. The characteristic band of TiO2 nanoparticles was observed to be slightly shifted to higher frequency at 630cm<sup>-1</sup>. Additionally, the characteristic band of paraffin wax was found at 2918cm<sup>-1</sup>.

## 3.1.2 (FT-IR) spectral data for nanocomposite [TiO2;ZnO/paraffin]by Ultra-sonic method.

The FT-IR spectrum of nanocomposite is shows (in Figure.2). The bands at 3743 cm<sup>-1</sup> (the vibratory stretch of OH) ,3612 cm<sup>-1</sup> (vibration stretching of C-H group), 1541 cm<sup>-1</sup> (bending vibration C=C), 1465 cm<sup>-1</sup> (CH<sub>3</sub> scissoring motion) and 1049 cm<sup>-1</sup> (C-O-C stretch vibration) were observed. The characteristic band of nanoparticles ZnO is found to be lightly shifted to the lower frequency at 424 cm<sup>-1</sup>. The characteristic band corresponding to the Ti-O bond in

the nanoparticles was observed to be slightly shifted towards a higher frequency at 619 cm-1. Additionally, the paraffin wax exhibited a band at 2918 cm-1.

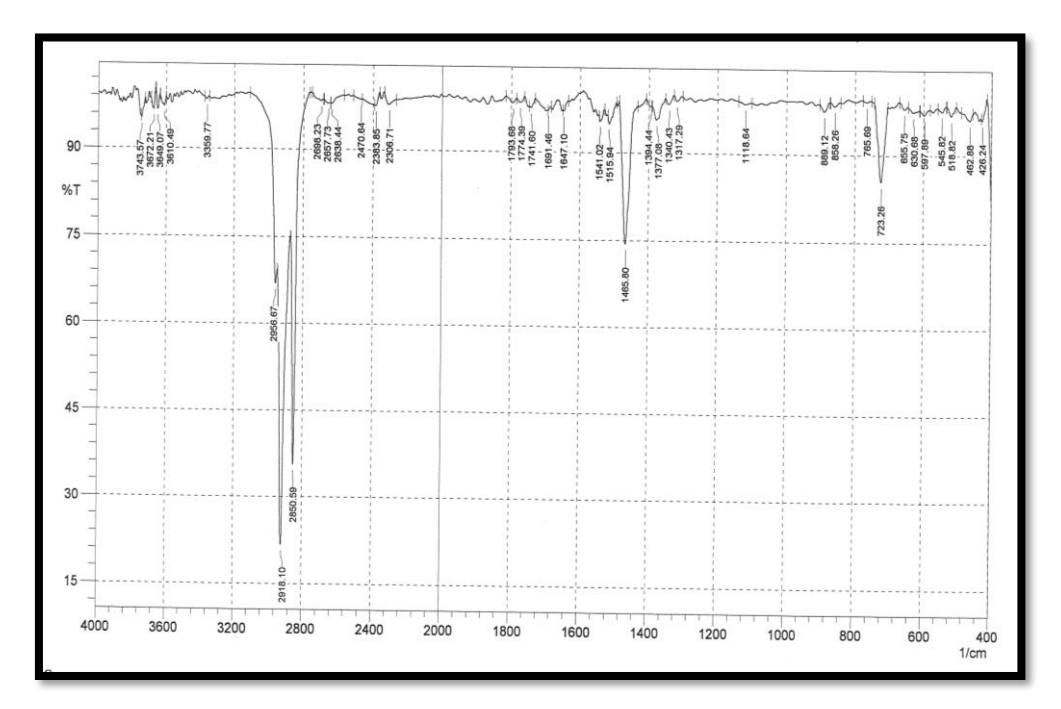
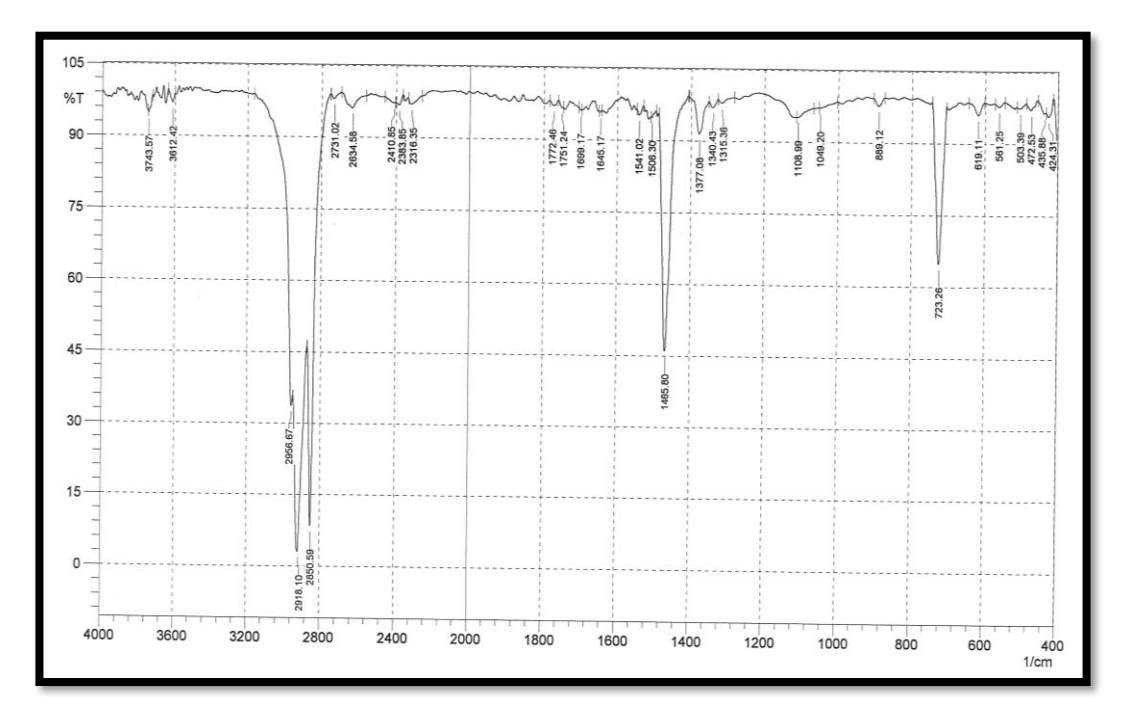


Figure 1: (FT-IR) spectrum for nanocomposite [TiO2;CuO/paraffin] using ultrasound.



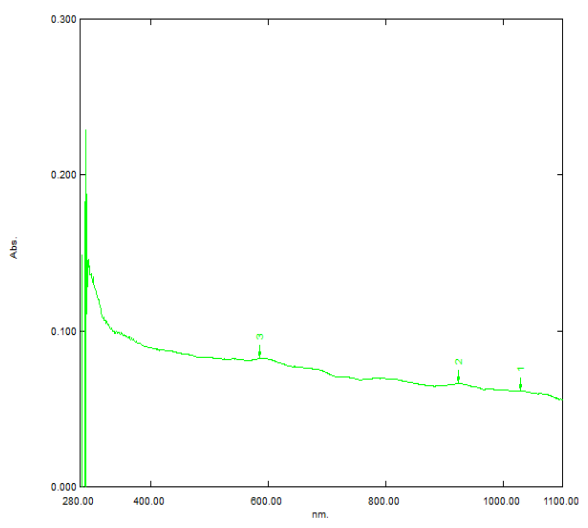
**Figure 2:** (FT-IR) spectrum for nanocomposite [TiO<sub>2</sub>;ZnO/paraffin] using ultrasound.

## 3.1.3 UV-Visible Spectroscopy

The absorbance spectrum of a substance in solution is obtained using ultraviolet-visible spectroscopy, electrons in a compound or material are stimulated from their ground state to their first singlet excited state by the absorption of electromagnetic radiation or light energy. The absorbance and wavelength for all synthesized nanocomposites were measured in chloroform at room temperature. The results are tabulated in (Table 1).

<b>Table 1:</b> The absorbance and	l wavelength for all	l synthesized nanocomposite.

compounds	Wavelength(nm) (Band position)	Absorbance	
IT'O . C . O / 6° . 1	1029.00	0.062	
	923.00	0.066	
[TiO2;CuO/paraffin]	585.00	0.082	
	258.00	2.353	
[T:O .7O/	931.00	0.011	
[TiO <sub>2</sub> ;ZnO/paraffin]	290.00	0.124	



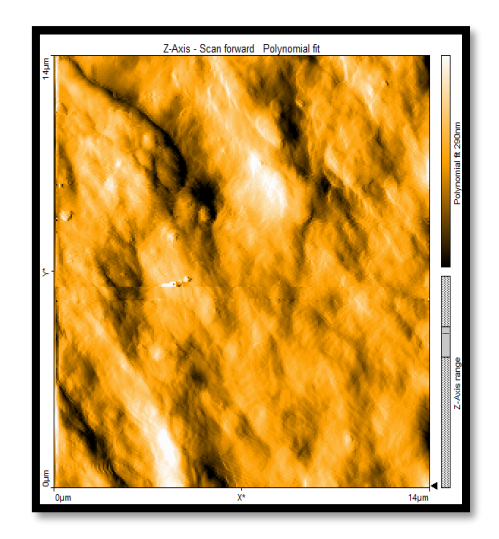
0.250 0.150 0.100 0.050 0.050 0.0000 0.000 0.000 0.000 0.000 0.000 0.000 0.000 0.000 0.0000 0.000 0.000 0.000 0.000 0.000 0.000 0.000 0.000 0.0000 0.000 0.000 0.000 0.000 0.000 0.000 0.000 0.000 0.0000 0.000 0.000 0.000 0.000 0.000 0.000 0.000 0.000 0.0000 0.000 0.000 0.000 0.000 0.000 0.000 0.000 0.000 0.0000 0.000 0.000 0.000 0.000 0.000 0.000 0.000 0.000 0.0000 0.000 0.000 0.000 0.000 0.000 0.000 0.000 0.000 0.0000 0.000 0.00000 0.0000 0.0000 0.0000 0.0000 0.0000 0.0000 0.0000 0.00000 0.00000 0

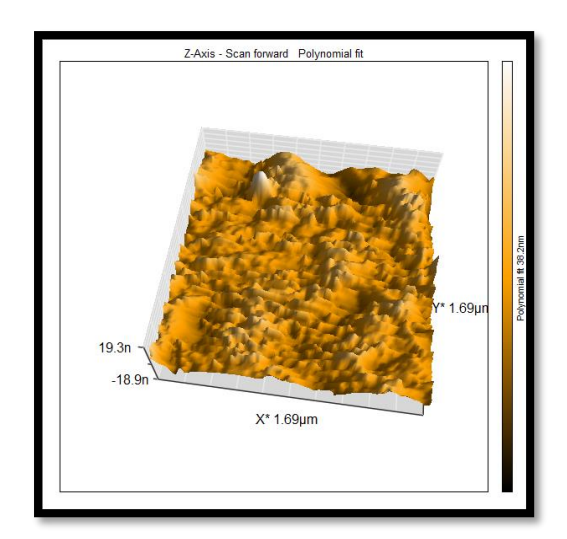
**Figure 3:** (UV-Vis) spectrum for nanocomposite [TiO<sub>2</sub>;CuO/paraffin] using ultrasound.

**Figure 4**. (UV-Vis) spectrum for nanocomposite [TiO<sub>2</sub>;ZnO/paraffin] using ultrasound.

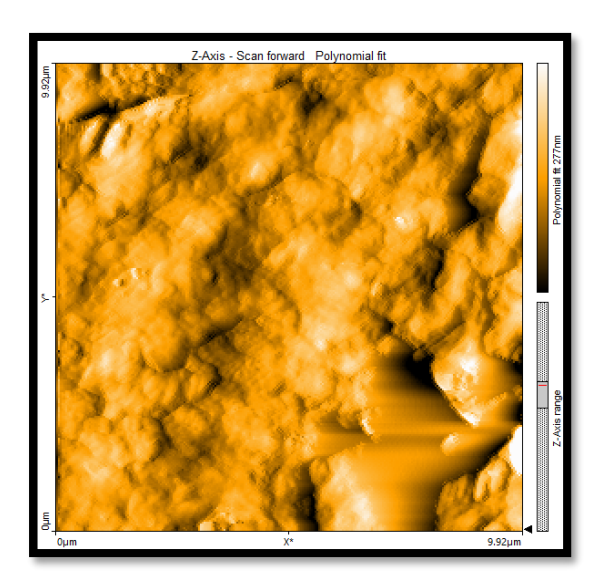
## 3.1.4Atomic force microscopy (AFM) for Nano composite by Ultra sonic method.

The AFM images of the paraffin/mixed metal oxide nanocomposite were captured in both two-dimensional (2D) and three-dimensional (3D) formats. In principle, the surface roughness of the films affects the films' structure and optical properties]. where the metal oxides consist from metals (Cu, Zn) as oxides (CuO, ZnO) with paraffin which reveals the topography, particle distribution and average diameter for all Nano composites synthesized via a chemical protocol (ultra -sonic method) which mentioned blow. Analysis of the [TiO2;CuO/paraffin] nanostructured composite via AFM revealed the average particle diameter to be 49.54 nm, as illustrated in Figure 5. The composite [TiO2; ZnO/paraffin] nanostructure showed that the particles' average diameter was 57.16 nm (in Figure.6).





**Figure 5:** (2D&3D) AFM images of nanocomposite [TiO<sub>2</sub>;CuO/paraffin].



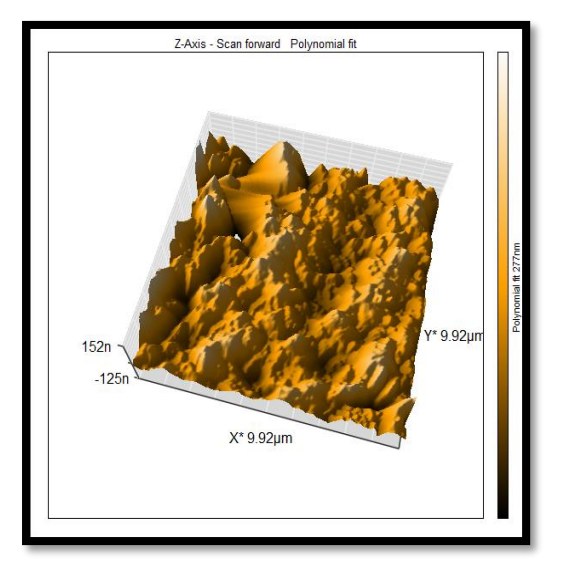


**Figure 6:** (2D&3D) AFM images of nanocomposite [TiO<sub>2</sub>;ZnO/paraffin].

### 3.1.5X-Ray diffraction of nanocomposite by Ultra-sonic method.

X-ray diffraction is currently a popular method for examining Atomic distance and crystal structures, It is used to identify the atomic arrangement, lattice parameters, and crystalline size A crystalline sample interacts positively with monochromatic X-rays to create X-ray diffraction, which is based on this interaction using the Denuded - Scherer formula [16]:

#### Where:

 $\mathbf{D}$  = the mean size(nm) of the ordered (crystalline).

 $\beta$  = half maximum intensity (FWHM).

 $\theta$  = angle (in radians).

 $\lambda = 0.15406$  nm (the X-ray wavelength).

 $\mathbf{K} = (\text{constant}) (0.9).$ 

XRD pattern of [TiO<sub>2</sub>;CuO/paraffin] nanostructure (see Figure.7) the peaks are to [TiO<sub>2</sub>;CuO/paraffin] which exhibited diffraction peaks at the 2θ values (22°, 31°, 34°, 39°,

41°,53°,58°, and 63°) which are assigned to (220), (400), (331), (422), (511), (533), (551),and(731) respectively. Crystalline phase cubic ,Standard JCPDS card number (00-049-0665). [17]. According to the analysis, the mean particle size of the [TiO2;CuO/paraffin] nanoparticles was found to be 30.11 nm.

XRD pattern of [TiO<sub>2</sub>;ZnO/paraffin] nanostructure(see Figure.8) the peaks are to [TiO<sub>2</sub>;ZnO/paraffin] which exhibited diffraction peaks at the 2θ values (23°, 25°, 30°, 33°, 38°,42°,53°, and 62°) which are assigned to (220), (211), (300), (310), (320), (400), (422), and(440) respectively. Crystalline phase cubic ,Standard JCPDS card number (00-039-0190) [18,19]. According to the analysis, the mean particle size of the [TiO<sub>2</sub>;ZnO/paraffin] nanoparticles was found to be 26 nm [TiO<sub>2</sub>;ZnO/paraffin].

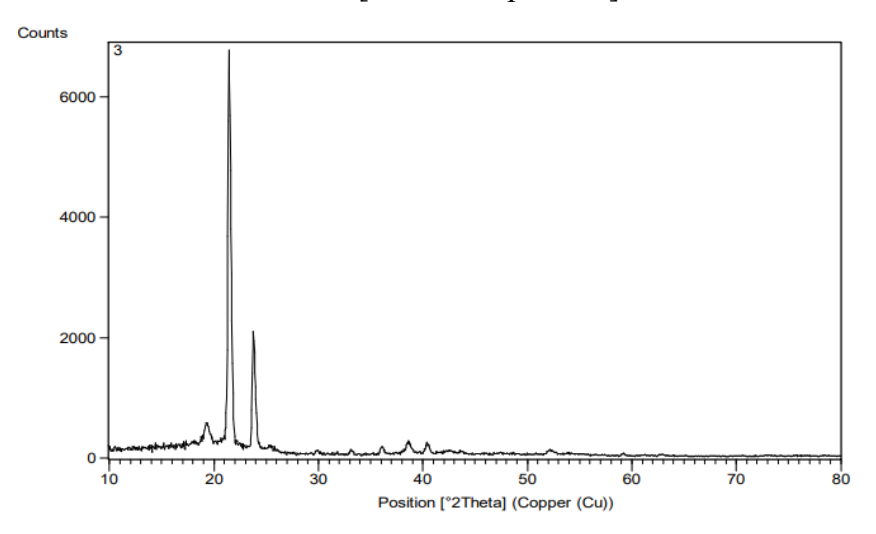


**Figure 7:** XRD pattern of [TiO<sub>2</sub>;CuO/paraffin] nanostructure using ultrasound

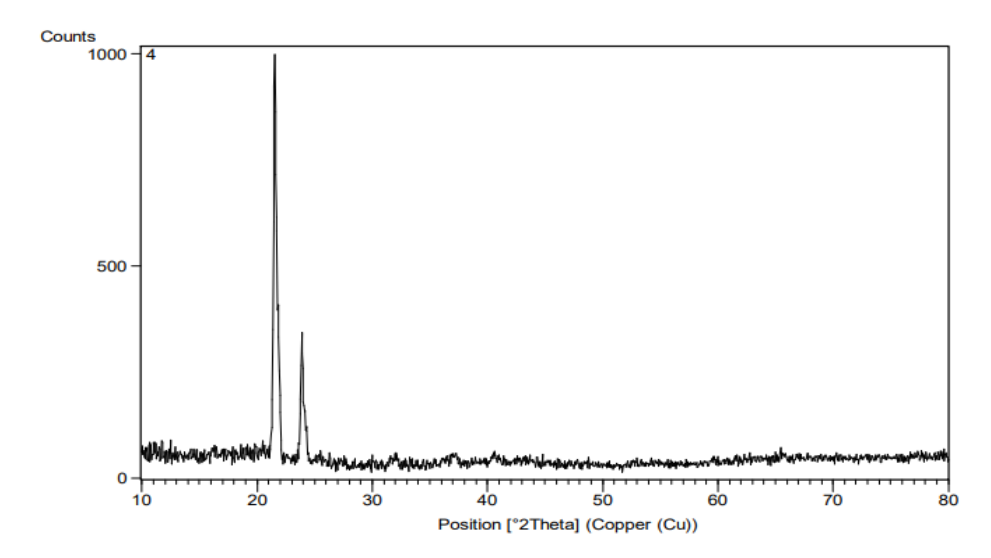


Figure 8: XRD pattern of [TiO<sub>2</sub>;ZnO/paraffin] nanostructure using ultrasound

## 3.3APPLICATIONS

#### 3.3.1- Solar cell energy

Fabrication of Dye-Sensitive Solar Cell (DSSCs)

The general components of DSSCs are dye-sensitizing[20] [ITO/TiO<sub>2</sub>; CuO/paraffin], photo-anodes based on metal oxides-doped paraffin (MxOX-P), [ITO/TiO<sub>2</sub>; ZnO/paraffin]

electrodes, counter electrodes, and electrolyte solution were made and assembled in a sandwich-like form (see Figure.9).



Figure 9: One of photo anode electrodes of nanocomposite after immersing in dye.

Table 2: Calculated energy conversion (PCE %) and full factor (ff) of DSSCs using ITO/

[TiO<sub>2</sub>;CuO/paraffin], ITO/ [TiO<sub>2</sub>;ZnO/paraffin].

cells	Voc/V	Isc/A Vmax/V		Imax/A	FF	P max/w	PCE%
[TiO2;CuO/paraffin]	0.760	0.0000693	0.4120	0.000029271	0.2289	0.000012060	2.4110
[TiO2;ZnO/paraffin]	0.096	0.0003333	0.0471	0.000166645	0.2432	0.000007849	1.5700

Table 2 presents the results, which indicate that paraffin wax is employed as a phase change material and a heat transfer fluid in this application, utilizing thermal storage systems to simulate a continuous flow of heat energy [21]. An approach to estimating storage system efficiency, The efficiency can be increased by using different metal oxides as nanoparticles to enhancement paraffin wax to achieve the best heat storage, thermal conductivity, and thermal stability, Paraffin wax thermal conductivity percentage increases with adding Nano CuO has been used as a hole transfer layer and barrier layer for dye-sensitized solar cells, CuO the efficiency in solar cell was 2.4110% is higher than another metal oxide, ZnO is a popular metal-oxide semiconductor for solar applications. They function as both an electron acceptor and a charge selective contact in solar cell hetero structures.

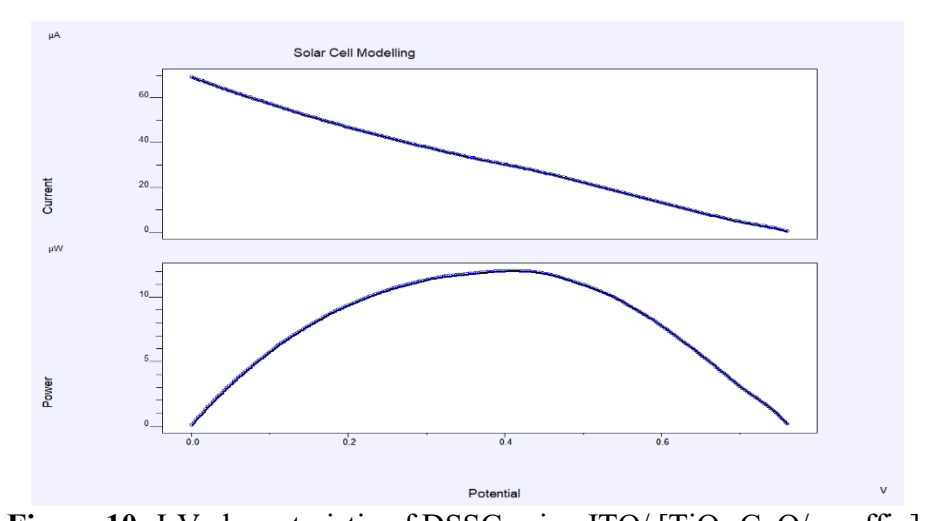


Figure 10: I-V characteristic of DSSC using ITO/ [TiO2;CuO/paraffin].

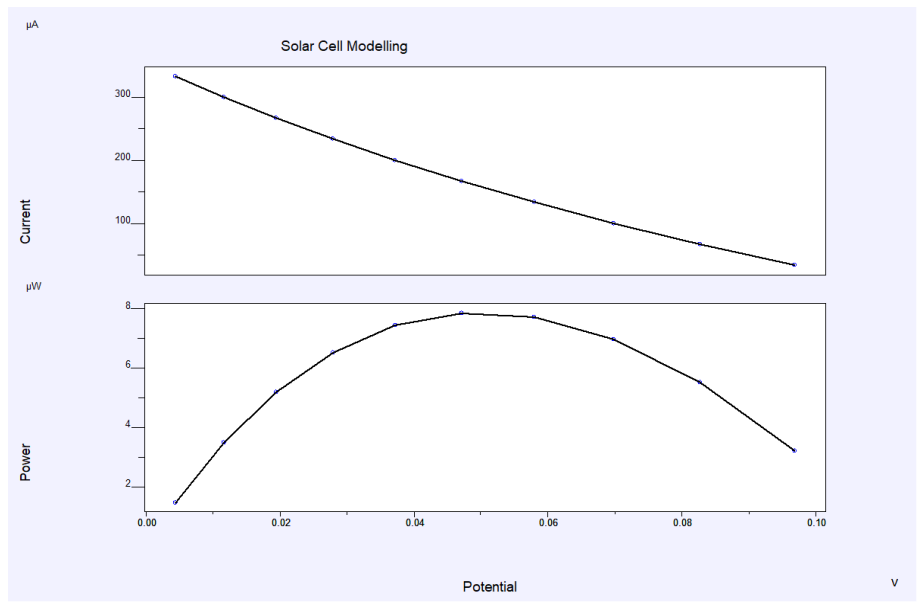


Figure 11: I-V characteristic of DSSC using ITO/[TiO<sub>2</sub>;ZnO/paraffin].

### 3.3.2 anti-Corrosion

Corrosion is the destructive attack of a metal by its reaction with the environment, depending on how a given metal is used a wide range of distinct ecosystems may be available. The situation where a bulk aqueous solution makes up the environment is the most typical. While the aqueous solution involved in atmospheric corrosion exists as a thin condensed layer rather than a bulk solution, the underlying principles remain largely similar.

**Table 3:** Corrosion parameters for blank (HCl) solution and different compounds [229,23,24].

Comp.	E corr.	I corr.	I corr./ r	Resis.	Anodi c β	Cathodic β	Corr. rate,	IE%
Blank	-0.527	163.5	3.269E-4	143.2	0.126	0.094	1.605	-
(TiO <sub>2</sub> ;paraffin /CuO)	-0.510	31.30	6.259E-5	2935	0.317	0.635	0.307	81
(TiO <sub>2</sub> ;paraffin/ NiO)	-0.544	16.41	3.282E-5	3230	0.185	0.359	0.161	90

The findings indicate improved paraffin/metal oxide corrosion resistance. This result is brought about by the metal's high metal affinity, which makes metal oxidation simple and creates a solid barrier to the surfaces of nanocomposites films. Overall findings show that higher metallic Nano oxide concentrations in the film were associated with increased corrosion protection efficacies.

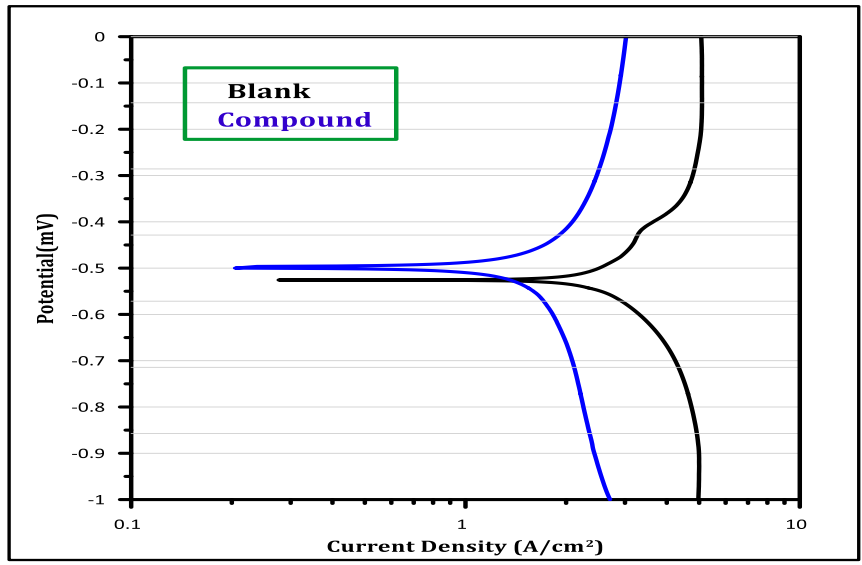


**Figure 10:** Polarization curves for corrosion of blank( HCl )solution and (TiO<sub>2</sub>;CuO/paraffin).

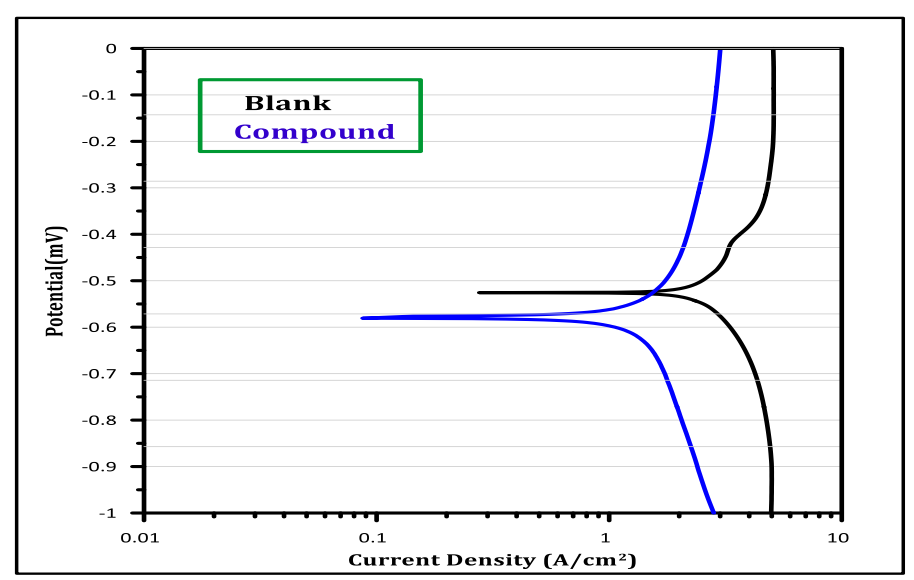


**Figure 11:** Polarization curves for corrosion of blank( HCl) solution and (TiO<sub>2</sub>;ZnO/paraffin ).

#### 4.Conclusion

In this study, metal oxide was prepared by hydrothermal method, and nanocomposite were prepared by ultra- sound method, All of synthesized nanocomposite were characterized using different techniques, and preparation Dye-Sensitized Solar Cell. The results of AFM for nanostructures prepared by ultra-sonic method were (49.54nm), (57.16nm), respectively for nanocomposite. The XRD results mean particle size for [TiO2;CuO/paraffin] nanoparticles have a crystal size of 30.11 nm and [TiO2;ZnO/paraffin] nanoparticles have a crystal size of 26 nm., The activities of nanocomposite synthesized were studied from the industrial side, including solar cell energy and the use of these nanocomposites as inhibitors for corrosion. The investigations into these nanocomposite revealed that they possess properties suitable for solar cell applications and exhibit a significant inhibitory effect.

## Acknowledgement

The authors would like to express their sincere gratitude to the consultant to all teaching staff in university of Baghdad, college of sciences for their valuable cooperation throughout thecourse of this study

#### References

- [1] J. Wang and S. Kaskel, "KOH activation of carbon-based materials for energy storage," *Journal of Materials Chemistry*, vol. 58, pp .35-37 ,2012.
- [2] S. Wang, C. Xiao and Y. Xing, "Carbon nanofibers/nanosheets hybrid derived from cornstalks as a sustainable anode for Li-ion batteries," *Journal of Materials Chemistry*, vol. 44, pp.37-38, 2015
- [3] Z. Abdin, M. Alim, A. Saidur, R. Islam and M. R. Rashmi, "Solar energy harvesting with the application of nanotechnology," *Journal of Renewable and Sustainable Energy*, vol. 26, pp 837–852,2018.
- [4] S. Komarneni, "Nanocomposites," Journal of Materials Chemistry, vol 2(12), pp.1219-1230,1992.
- [5] P.H.C. Camargo, K.G. Satyanarayana and F. Wypych, "Nanocomposites: synthesis, structure, properties and new application opportunities," *Journal of Materials Research*, vol. 12, pp.1-39,2009.
- [6] H. Gleiter, "Materials with ultrafine microstructures: Retrospectives and perspectives," *Journal of Nanostructured Materials*, vol.1, pp.1-19,1992
- [7] M.Ventra, S. Evoy and J.R. Heflin, "Introduction to nanoscale science and technology," *Springer Science & Business Media*,vol.7,pp.204-219, 2006
- [8] S. Bhatiaa and S. Bhatia, "Nanoparticles types, classification, characterization, fabrication methods and drug delivery applications," *Journal of Natural Polymer Drug Delivery Systems: Nanoparticles, Plants, and Algae*, vol. 66, pp.33-93, 2016.
- [9] S. Pina, J.M. Oliveira and R.L. Reis, "Natural-based nanocomposites for bone tissue engineering and regenerative medicine," *Journal of review Advanced Materials*, vol. 27(7), p. 1143-1169, 2015.
- [10] D. Afzali and M. Fayazi, "Deposition of MnO2 nanoparticles on the magnetic halloysite nanotubes by hydrothermal method for lead (II) removal from aqueous solutions," *Journal of the Taiwan Institute of Chemical Engineers*, vol. 63, pp.421-429, 2016.
- [11] L. Y. Meng, B. Wang and K.L. Lin, "The progress of microwave-assisted hydrothermal method in the synthesis of functional nanomaterials," *Journal of Materials Today Chemistry*, vol. 1, pp.63-83, 2016.
- [12] J.A. Fuentes-García, J. Santoyo-Salzar, E. Rangel-Cortes, G.F.Goya, V.Cardozo-Mata and J.A. Pescador-Rojas, "Effect of ultrasonic irradiation power on sonochemical synthesis of gold nanoparticles," *Journal of Ultrasonics Sonochemistry*, vol.70, p.105274, 2021.
- [13] A. Elengoe and S. Hamdan, "Heat sensitivity between human normal liver (WRL-68) and breast cancer (MCF-7) cell lines," *Journal of Biotechnology*, vol. 5,pp.7-8, 2013.
- [14] G. Gopalakrishnan, "Antibacterial activity of Cu<sub>2</sub>O nanoparticles on E. colisythesised from tridax procumbens leaf extract and surface coating with polyaniline Digest," *Journal of Nanomaterials and Biostructures*, vol.7, pp.10-13, 2012.
- [15] P. Andreeva, V. Stoilov and O. Petrov, "Application of X-ray Diffraction Analysis for Sedimentological Investigation of Middle Devonian Dolomites from Northeastern Bulgaria," *Journal of Geologica Balcanica*,vol.40,pp.31-38, 2011.
- [16] A.A.Radhakrishnan and B.B. Beena, "Structural and Optical Absorption Analysis of CuO Nanoparticles," *Indian Journal of Advances in Chemical Science*,vol.9,pp.55-60, 2014.
- [17] B.D. Hall, D. Zanchet and G.Ugarte, "Estimating Nanoparticle Size from Diffraction Measurements," *Journal of Powder Diffraction*, vol. 33, pp.1335-1341. 2000.
- [18] B. B. He, "Introduction to two-dimensional X-ray diffraction," *Journal of Powder Diffraction*, vol. 18, pp.50, 2003.

- [19] W. wang, "Dye-Sensitized vs. Thin Film Solar Cells," Journal *European Institute for Energy Research*, vol.12, pp.40-47, 2006.
- [20] H.Hajare and B.S. Gawali, "Experimental study of latent heat storage system using nano-mixed phase change material," *International Journal of Engineering Technology, Management and Applied Sciences*, vol. 03(08), pp. 37–44, 2015.
- [21] D. L. Graver, "Corrosion Data Survey, Metals Section," NACE, Houston, TX (1985). (Available as an electronic book as "Corrosion Survey Database" by Knovel Corporation, Norwich, NY, 2002.
- [22] A.M. Al-Azzawi and H.K. Yaseen, "Synthesis, characterization and polymerization of new maleimides," *Journal of Pharmaceutical Rescerch*, vol. 8, pp. 241-247, 2016.
- [23] A.M. AL-Sammarraie, "Role of carbon dioxide on the corrosion of carbon steel reinforcing bar in simulating concrete electrolyte," *Baghdad Science Journal*, vol.17,pp. 0093-0093, 2020.
- [24] E. Heitz and W. Schwenk, "Theoretical basis for the determination of corrosion rates from polarisation resistance: Report prepared for the european federation of corrosion working party on 'physicochemical testing methods of corrosion—fundamentals and application," *British Corrosion Journal*, vol.11,pp. 74-77, 1976.
- [25] F.A.Al-jubouri and B.I.Al-Abdaly, "Cu-ZnO Nanostructures Synthesis and Characterization," *Iraqi Journal of Science*, vol. 62(3), pp. 708-717, 2021.
- [26] H.M.Al-saidi, H.H.Hadi and W.W.Hasan, "Preparation and Characterization of ZnO Nano-Sheets Prepared by Different Depositing Methods," *Iraqi Journal of Science*,vol. 63(2),pp. 538-547, 2022.
- [27] D.D.Maki and S.S.Najem, "Use of Nano Chemical Additives to Improve the Properties of Industrial Used Paraffin Wax," *Iraqi Journal of Science*, vol.64, pp. 99-104, 2019.
- [28] A.A.Jasim, A. Aadim and S.S.Naji, "Optical and Structural Properties of Cobalt Nanoparticles Synthesized by Laser Ablation," *Iraqi Journal of Science*, vol 63(10),pp. 4292-4304, 2022.
- [29] I. Q. Kaddou and K. A. Al-Horani, "Mixtures of beeswax and paraffin their importance in bee culture and their role," *Baghdad Science Journal*, vol. 2, pp. 533–538, 2021.